Neuron, Vol. 48, 101–114, May 4, 2005 ©2005 Elsevier Inc. DOI 10.1016/j.neuron.2005.08.034

Activity-Induced Rapid Synaptic Maturation Mediated by Presynaptic Cdc42 Signaling

Wanhua Shen,[1,2,5] Bei Wu,[1,2,5] Zhijun Zhang,[1,2] Ying Dou,[1,2] Zhi-ren Rao,[3] Yi-ren Chen,[1,4] and Shumin Duan[1,*]

[1] Institute of Neuroscience and
Key Laboratory of Neurobiology
Shanghai Institutes for Biological Sciences
Chinese Academy of Sciences
Shanghai 200031
China

[2] Graduate School of the Chinese Academy of Sciences
Shanghai 200031
China

[3] Institute of Neuroscience
The 4th Military Medical University
Xian
China

[4] Institute of Neuroscience Research
Nantong University
Nantong, Jiangsu
China

Summary

Maturation of presynaptic transmitter secretion machinery is a critical step in synaptogenesis. Here we report that a brief train of presynaptic action potentials rapidly converts early nonfunctional contacts between cultured hippocampal neurons into functional synapses by enhancing presynaptic glutamate release. The enhanced release was confirmed by a marked increase in the number of depolarization-induced FM4-64 puncta in the presynaptic axon. This rapid presynaptic maturation can be abolished by treatments that interfered with presynaptic BDNF and Cdc42 signaling or actin polymerization. Activation of Cdc42 by applying BDNF or bradykinin mimicked the effect of electrical activity in promoting synaptic maturation. Furthermore, activity-induced increase in presynaptic actin polymerization, as revealed by increased concentration of actin-YFP at axon boutons, was abolished by inhibiting BDNF and Cdc42 signaling. Thus, rapid presynaptic maturation induced by neuronal activity is mediated by presynaptic activation of the Cdc42 signaling pathway.

Introduction

The formation and maturation of synaptic connections during early development follow a strict time course and are regulated by neuronal activity (Lee and Sheng, 2000; Renger et al., 2001; Ziv and Garner, 2004). Nonfunctional synaptic contacts, known as silent synapses, are frequently found in various brain regions during development (Atwood and Wojtowicz, 1999; Choi et al., 2003; Gasparini et al., 2000; Kullmann and Asztely, 1998; Nicoll, 2003; Renger et al., 2001). Although intensively studied within the context of synaptic plasticity, the property of silent synapses during synaptogenesis and mechanisms responsible for their conversion into functional ones remain largely unknown. The popular notion of glutamatergic silent synapses refers to synapses containing postsynaptic NMDA receptors (NMDARs) but not AMPA receptors (AMPARs). These synapses are nonfunctional under normal physiological conditions because of voltage-dependent Mg^{2+} block of NMDARs. Activity-dependent persistent enhancement of synaptic transmission, known as long-term potentiation (LTP), has been attributed to the unsilencing of these silent synapses through trafficking of AMPARs to the postsynaptic membrane (Malinow and Malenka, 2002; Nicoll, 2003). However, it is possible that some silent synapses are not due to the lack of postsynaptic AMPARs, but caused by a deficiency in presynaptic release (Berninger et al., 1999; Choi et al., 2003; Kullmann and Asztely, 1998; Renger et al., 2001). Such presynaptic silent synapses may be also converted into full functional ones through developmental or activity-dependent presynaptic maturation, but the underlying molecular mechanisms are unknown.

One of the critical steps in activity-dependent synaptic modification is a reorganization of the actin cytoskeleton (Carlisle and Kennedy, 2005; Colicos et al., 2001; Dillon and Goda, 2005; Doussau and Augustine, 2000; Matus, 2000). While activity-dependent actin dynamics and remodeling at postsynaptic spines have received much attention (Carlisle and Kennedy, 2005; Matus, 2000), the role of actin rearrangement in the presynaptic modification is less clear (Colicos et al., 2001; Dillon and Goda, 2005; Sankaranarayanan et al., 2003). Actin cytoskeleton in many cell types is under the regulation of the Rho family GTPases, including RhoA, Rac, and Cdc42 (Hall, 1998), all of which are present in rat brain synaptosomes (Doussau et al., 2000). Actin polymerization evoked by Cdc42 is involved in the BDNF-induced axon guidance (Yuan et al., 2003) and in the learning-related synaptic growth in *Aplysia* sensory neurons induced by prolonged treatment with 5-HT (Udo et al., 2005). However, it is unclear whether Cdc42 signaling also plays a role in the activity-induced rapid synaptic maturation and plasticity.

Synapses between cultured hippocampal neurons develop in a stereotypic and synchronous manner, providing an ideal system for studying synapse maturation (Lee and Sheng, 2000; Renger et al., 2001; Ziv and Garner, 2004). Using paired whole-cell recordings that permit us to analyze and manipulate separately the properties of either pre- or postsynaptic neurons, we found that in cultures younger than 10 day in vitro (DIV), there was a high frequency of cell-cell contacts that lack both AMPAR- and NMDAR-mediated synaptic responses, even in the Mg^{2+}-free solution. Consistent with previous report (Renger et al., 2001), we found that a large proportion of presynaptic terminals, as defined by immunostaining of the synaptic vesicle-associated protein synaptophysin (SNP), did not

*Correspondence: shumin@ion.ac.cn
[5] These authors contributed equally to this work.

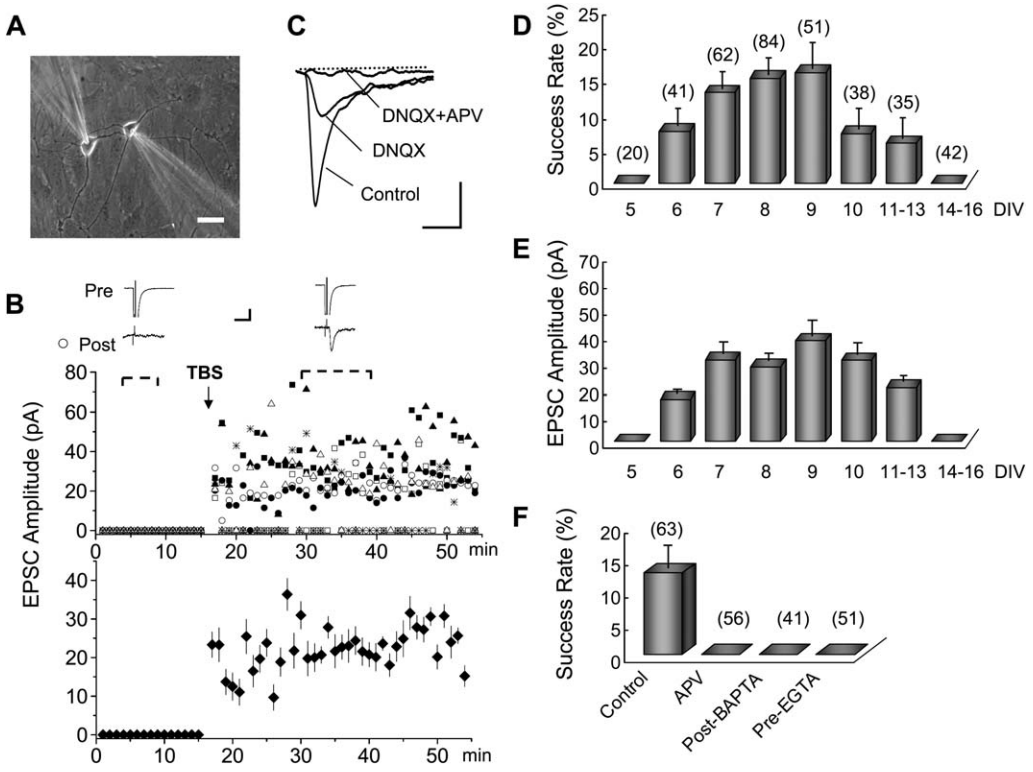

Figure 1. Conversion of Silent Synapses by TBS

(A) Phase-contrast image showing dual patch recording from cultured neurons for detection and induction of functional synaptic transmissions. Scale bar, 10 μm.

(B) Upper panel: Examples recordings from seven pairs of cultured neurons (7–9 DIV) showing that evoked EPSCs were recorded immediately after TBS application to the presynaptic neuron. Each type of symbol represents data from one neuron. Note some failures in evoked EPSCs after TBS application. Lower panel: Time course of the averaged amplitude of EPSCs from recordings shown in the upper panel. Insets are example recordings of membrane currents from the pair indicated by the open circle. The responses were averaged during the period indicated by dashed lines, showing presynaptic application of a test pulse (+30 mV, 2 ms) evoked presynaptic Na^+ currents (pre) and postsynaptic responses (post) before (left trace) and after (right trace) TBS application. The amplitude of Na^+ currents was truncated. Scales in insets: 100 (pre) and 10 (post) pA, 5 ms.

(C) Example averaged EPSCs recorded in a 7 DIV neuron showing that TBS-induced functional synaptic transmission contains both AMPAR and NMDAR components. Scales: 10 pA, 5 ms.

(D) Summarized data showing the success rate in TBS-induced functional synapses tested in neurons of different developmental stages.

(E) Averaged EPSC amplitudes of TBS-induced functional synapses in neurons of different developmental stages as shown in (D).

(F) Summary of data showing the effects of various treatments on the success rate in TBS-induced conversion of silent synapses tested in 7–9 DIV neurons. The number associated with each column in (D) and (F) refers to the number of cell pairs tested in each condition.

Error bars show SEM.

undergo loading of the active synapse marker FM4-64 in young cultures (6–9 DIV), indicating that these synapses are nonfunctional presynaptically. We found that such silent synapses can be rapidly converted to functional ones by a brief theta bursting stimulation (TBS) of the presynaptic, but not the postsynaptic, cell. Further studies showed that the activity-induced rapid unsilencing of these presynaptically deficient synapses involves presynaptic activation of TrkB receptors by BDNF and subsequent activation of Cdc42 signaling, leading to the remodeling of actin cytoskeleton that may be required for presynaptic maturation.

Results

Rapid Conversion of Silent Synapses into Functional Ones by Presynaptic Activity

Formation of functional synapses between hippocampal neurons was examined by dual whole-cell recording from cell pairs cultured from E18 rat hippocampi (Zhang et al., 2003). Excitatory postsynaptic synaptic currents (EPSCs) evoked by presynaptic stimulation with a brief step depolarization (to +30 mV, 2 ms) were monitored in Mg^{2+}-free extracellular solution containing 1 μM glycine. In young cultures (6–9 DIV), few neuronal pairs (Figure 3D, 22% ± 2.21%, n = 218) exhibited functional synaptic transmission. However, in a fraction of the nonfunctional pairs, we found that application of a brief train of TBS to one cell resulted in an immediate appearance of functional synaptic transmission, as shown by EPSCs recorded in the other cell (Figure 1B). Interestingly, TBS was effective in triggering the conversion only when it was applied to the presynaptic partner of the cell pair. The rate for TBS-induced conversion of silent synapses depended on the developmental stage of the culture. For neurons younger than 6 DIV, no functional synapse was induced by TBS. At 6 DIV, EPSCs could be detected in about 8% of recorded nonfunctional pairs after TBS

stimulation. The success rate of induction reached the peak at 8–9 DIV (~16%). For cultures older than 10 DIV, when EPSCs could be recorded frequently without TBS stimulation, the success rate for TBS-induced unsilencing became greatly decreased. No conversion of silent synapses could be induced by TBS in cultures older than 14 DIV (Figures 1D and 1E). For the following experiments we used 7–9 DIV cultures except where noted.

The EPSCs recorded from TBS-induced functional synapses are mediated by both NMDARs and AMPARs, since perfusion of the AMPAR antagonist DNQX (6-cyano-7-nitroquinoxaline-2, 3-dione, 10 μM) reduced the amplitude of EPSCs by more than 70%, and the residual EPSC with slow kinetics was abolished by adding the NMDAR antagonist APV (D, L-2-amino-5-phosphonovaleric acid, 50 μM, Figure 1C). The average ratio of NMDAR to AMPAR components of the EPSCs for TBS-induced functional synapses was 0.26 ± 0.06 (n = 6). The conversion of silent synapses depends on the activation NMDARs, since it was abolished by APV (50 μM). Furthermore, loading of the postsynaptic cell with the fast Ca^{2+} chelator BAPTA [1,2-bis (2-aminophenoxy) ethane-N,N,N′,N′-tetraacetic acid, 10 mM] through the recording pipette led to a complete absence of conversion to functional transmission in all cell pairs tested (n = 41), suggesting that postsynaptic elevation of Ca^{2+} is required for the conversion. Presynaptic loading of a slow Ca^{2+} chelator EGTA [ethylene glycol-bis (2-aminoethyl-ether)-N,N,N′,N′-tetraacetic acid, 20 mM], which does not block transmitter release, also abolished the TBS-induced conversion (Figure 1F). Thus, both pre- and postsynaptic Ca^{2+} is critical for TBS-induced conversion.

Endogenous BDNF Is Required for TBS-Induced Conversion

BDNF is known to play an important role in synaptogenesis and synaptic plasticity (Berninger et al., 1999; Itami et al., 2003; Korte et al., 1995; Kovalchuk et al., 2002; Li et al., 1998; Lu, 2003; Vicario-Abejon et al., 1998; Zakharenko et al., 2003). Furthermore, endogenous BDNF is required for the TBS-induced presynaptic component of LTP in hippocampal CA3-CA1 synapses (Zakharenko et al., 2003) and the TBS-induced increase in FM dye-labeled functional presynaptic terminals in hippocampal cultures (Slutsky et al., 2004). To examine whether BDNF is involved in the TBS-induced rapid conversion of silent synapses to functional ones, we added a BDNF antibody (10 μg/ml) in the extracellular solution to neutralize endogenously released BDNF. We found that TBS failed to induce functional transmission in all cell pairs examined in the presence of the BDNF antibody (Figure 2D). In addition, bath application of tyrosine kinase inhibitor K252a, which inhibits BDNF-TrkB signaling, also abolished TBS-induced conversion. To examine the site of BDNF action, we transfected neurons with a construct expressing eGFP-linked truncated TrkB (TrkB·T1), which lacks tyrosine kinase activity and serves as dominant-negative suppression of endogenous TrkB signaling (Li et al., 1998). When TBS-induced conversion of nonfunctional synapses between control (nontransfected) and TrkB·T1-transfected neurons was examined 24–48 hr after transfection, we found that conversion only occurred when TBS was applied to the untransfected but not to the transfected neuron of the cell pairs (Figures 2B and 2D), suggesting that activation of presynaptic TrkB is critical for TBS-induced conversion. Neurons transfected with eGFP, either pre- or postsynaptically, did not affect TBS-induced conversion (Figure 2D). On the other hand, synaptic transmission was still recorded from some neuronal pairs (in the absence of TBS) expressing TrkB·T1 either pre- or postsynaptically (data not shown), suggesting that TrkB·T1 expression did not abolish synaptic transmission of mature synapses. Finally, we found that the presence of BDNF by itself was sufficient for the conversion of silent synapses. As shown in Figures 2C and 2D, perfusion with BDNF (100 ng/ml) induced conversion of silent synapses into functional ones in 5 out of 46 tested pairs (11%). Similar to the TBS-induced functional synapses, BDNF-induced conversion was also prevented by the APV treatment or by loading EGTA into either pre- or postsynaptic neurons. Furthermore, TBS did not induce functional synapses in pairs that failed to respond to BDNF perfusion (BDNF failure, Figure 2D), suggesting that similar mechanisms are involved in the conversion by these two stimuli.

Involvement of Presynaptic Cdc42 Signaling

BDNF has been reported to activate the small GTPase Cdc42 (Yuan et al., 2003). To examine whether this signaling transduction pathway is involved in TBS-induced functional synapses, we treated cultures with Toxin B (10 μg/ml for 30 min), a general inhibitor of Rho family GTPases. Such treatment completely abolished TBS-induced conversion (Figure 3C), although synaptic transmission was still observed at mature synapses (Figures 3D and 3E). To block Cdc42 signaling specifically without affecting other Rho GTPases, neurons were transfected with eGFP-linked dominant-negative Cdc42 (DN-Cdc42) that suppresses the activity of endogenous Cdc42 through competitive and irreversible binding to guanine nucleotide-exchange factor of Cdc42, the upstream regulators of the GTPase (Udo et al., 2005; Yuan et al., 2003). TBS-induced conversion was then examined at nonfunctional contacts formed between control and DN-Cdc42-expressing neurons 24–48 hr after the transfection. We found that transfection with DN-Cdc42 in presynaptic but not in postsynaptic neurons abolished TBS-induced conversion (Figures 3A and 3C). The synaptic transmission was still observed in some cell pairs in the absence of TBS, regardless of whether DN-Cdc42 was expressed in the pre- or postsynaptic neuron of these pairs (Figures 3D and 3E). Furthermore, conversion of silent synapses to functional ones by direct perfusion of BDNF was also abolished by the presynaptic, but not postsynaptic, cell transfection with DN-Cdc42 (Figure 3C), suggesting that Cdc42 is a downstream effector of BDNF. On the other hand, transfection in either pre- or postsynaptic cells with eGFP-linked dominant-negative Rac (DN-Rac), another Rho GTPase family member that is functionally related to Cdc42 and known to regulate spine morphology, synaptogenesis, and transmitter release (Humeau et al., 2002; Zhang et al., 2005), did not affect TBS-induced conversion (Figure 3C). Finally, to further test whether activation of Cdc42 signal alone can induce functional synapses,

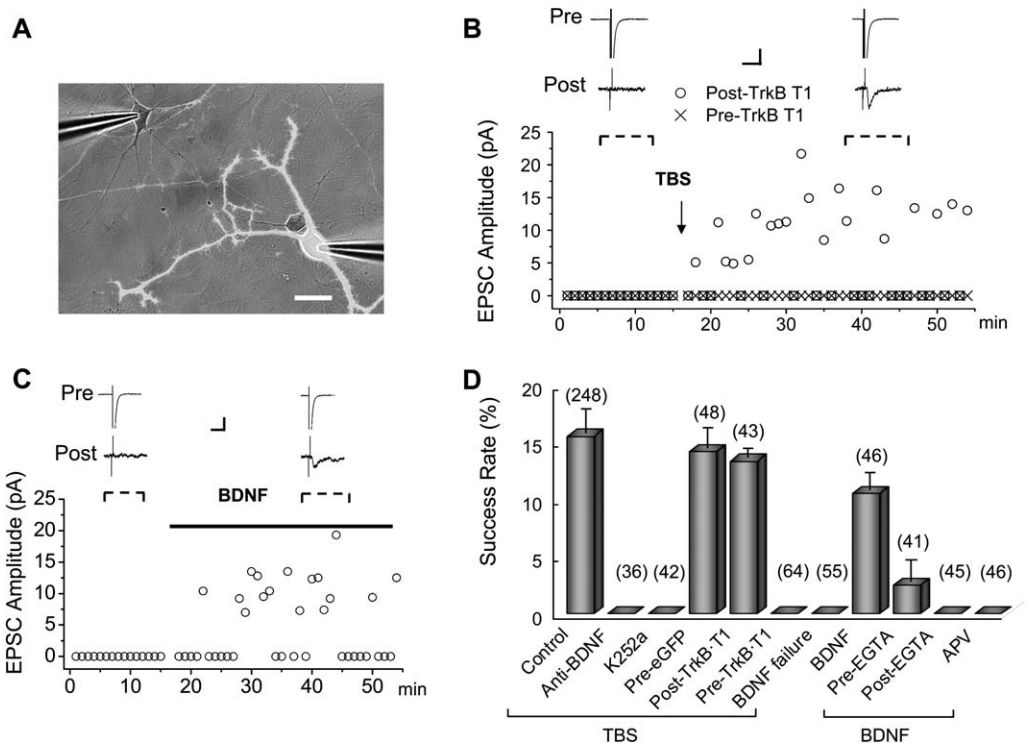

Figure 2. Involvement of BDNF Signaling in the Activity-Induced Conversion of Silent Synapses

(A) Superimposed phase-contrast and fluorescent images showing an example of dual patch recordings from a control neuron (left, gray) and a neuron transfected with GFP-linked TrkB·T1 receptor (right, white). Scale bar, 10 μm.

(B) Example recordings showing that TBS can induce functional synaptic transmission when TrkB·T1 receptor was transfected into postsynaptic neuron (open circles, Post-TrkB·T1), but not when transfected into presynaptic neuron (crosses, Pre-TrkB·T1). Insets are recorded membrane currents averaged from data points indicated by dashed lines, showing evoked Na^+ current at presynaptically nontransfected neuron (upper traces) and response in a postsynaptic neuron (lower traces) transfected with TrkB·T1 before (left trace) and after (right trace) TBS.

(C) Example recording showing that direct perfusion of BDNF (100 ng/ml, indicated by the bar) rapidly induced functional synaptic transmission without TBS application. Insets are recorded membrane currents averaged from data points indicated by dashed lines, showing evoked presynaptic Na^+ current and postsynaptic responses before (left trace) and during (right trace) BDNF perfusion.

(D) Summarized data showing effects of various treatments on the success rate of TBS- or BDNF-induced functional synaptic transmission. Anti-BDNF, cultures treated with BDNF antibody (10 μg/ml). Pre-eGFP, presynaptic neuron transfected with eGFP. BDNF failure, pairs failed to exhibit conversion by perfusion of BDNF. Pre-EGTA and Post-EGTA, loading EGTA through the recording pipette into the pre- and postsynaptic neuron, respectively. The number associated with each column refers to the number of cell pairs tested in each condition.

Scales in (B) and (C): 100 (pre) and 10 (post) pA, 5 ms. Error bars show SEM.

we applied another Cdc42 activator, bradykinin (Kozma et al., 1995), to these cultures. We found that perfusion of bradykinin alone (without TBS) also induced conversion of silent synapses rapidly (Figures 3B and 3C), an effect that can be abolished by presynaptic, but not postsynaptic, transfection with DN-Cdc42 (Figure 3C). Thus, Cdc42 signaling is not only necessary but is also sufficient for the rapid induction of functional synapses. Activation of Cdc42 signaling plays a critical role in actin polymerization in the neuronal growth cone (Hall, 1998). We then examined whether TBS-induced functional synapses requires actin polymerization. As shown in Figure 3C, treatment of cultures with the actin-depolymerizing agent cytochalasin D (Cyt D, 2 μg/ml, 30 min) abolished TBS-induced conversion of silent synapses.

Cdc42 Is Critical for TBS-Induced LTP in Young Cultures

Functional synapses were recorded from some young cultures (7–9 DIV) in the absence of TBS stimulation (Figure 3D). Presynaptic application of TBS in cell pairs with functional synapses in young cultures resulted in a rapid and persistent increase in the amplitudes of EPSCs (Figure 4), in a manner similar to that of LTP. This TBS-induced synaptic potentiation was not found in old cultures. Furthermore, transfection of the culture with DN-Cdc42 in presynaptic, but not in postsynaptic, neurons prevented TBS-induced synaptic potentiation in young cultures (Figure 4), indicating that Cdc42 signaling is also critical for this form of synaptic plasticity in young cultured neurons. It is possible that in young cultures TBS converted some silent synapses in these cell pairs that had already established functional synaptic connections.

Rapid Induction of Active Presynaptic Terminals

The above results obtained from neurons transfected with DN-Cdc42 or TrkB·T1 showed that TrkB and Cdc42 signaling in the presynaptic neuron is critical for the TBS- or BDNF-induced conversion of silent synapses to functional ones. To further clarify whether this conversion results from rapid changes in presynaptic

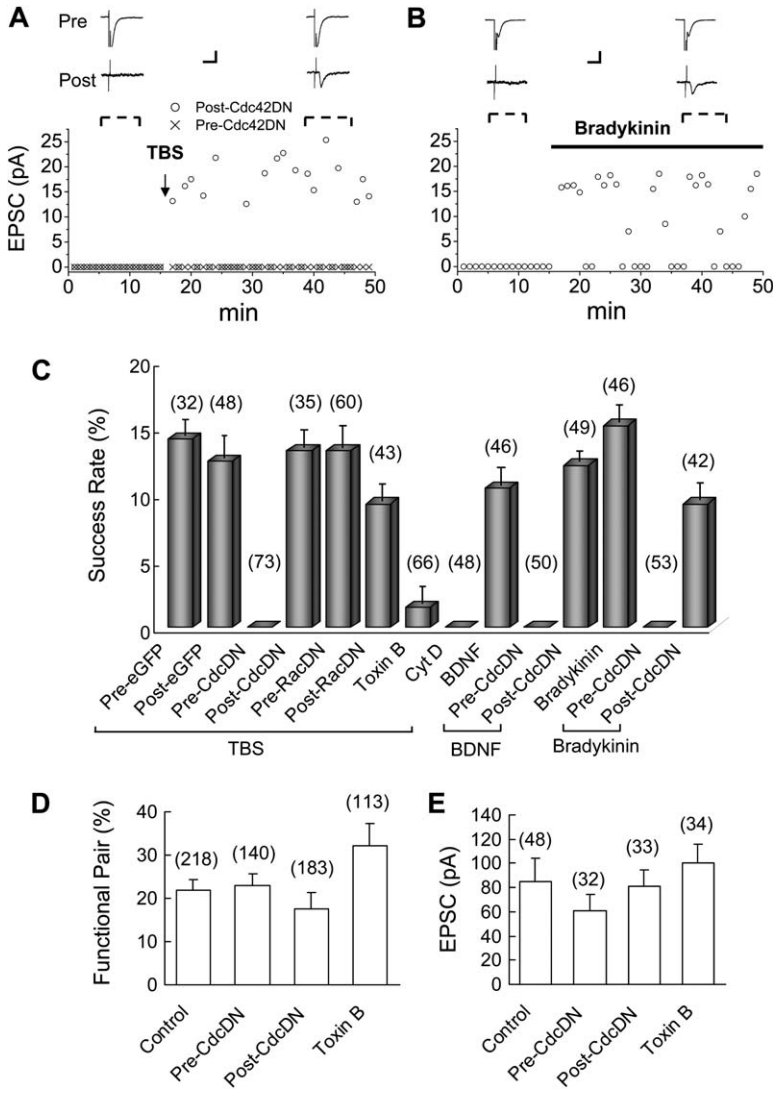

Figure 3. Involvement of the Cdc42 Signaling in the Activity-Induced Rapid Conversion of Silent Synapses

(A) Example recording showing that TBS-induced functional synaptic transmission was blocked by the presynaptic (crosses, Pre-Cdc42DN), but not by the postsynaptic (open circles, Post-Cdc42DN) transfection of DN-Cdc42. Insets are recorded membrane currents averaged from data points indicated by dashed lines, showing evoked Na^+ current at presynaptic nontransfected neuron (upper traces) and response at postsynaptic neuron (lower traces) transfected with DN-Cdc42 before (left trace) and after (right trace) TBS.

(B) Example recording showing that direct perfusion of Cdc42 activator bradykinin (100 ng/ml) rapidly induced functional synaptic transmission without TBS application. Insets are recorded membrane currents averaged from data points indicated by dashed lines, showing evoked Na^+ current at presynaptic neuron (upper traces) and response at postsynaptic neuron (lower traces) before (left trace) and during (right trace) bradykinin perfusion.

(C) Summary of data showing effects of various treatments on the success rates of TBS-, BDNF-, and bradykinin-induced functional transmission.

(D) Percent of recorded pairs exhibiting functional synaptic connections without induction under various conditions. No significant difference was found in different groups.

(E) Averaged EPSC amplitudes of basal synaptic connections (without induction) as shown in (D). No significant difference was found in different groups. The number associated with each column in (C) to (E) refers to the number of cell pairs tested in each condition. Scales in (A) and (B): 100 (pre) and 10 (post) pA, 5 ms. Error bars show SEM.

transmitter release machinery or postsynaptic receptor responses, we examined whether electric field stimulation (EFS) and BDNF can rapidly upregulate the number of active presynaptic terminals, as defined by FM dye (FM4-64)-labeled fluorescent puncta that can be destained by high K^+-induced depolarization (Renger et al., 2001; Slutsky et al., 2004). Consistent with previous report (Slutsky et al., 2004), EFS (three trains of 50 Hz, 1 ms pulses, with each train consisting of 300 pulses, the polarity was reversed after each train with a 10 s interval) of the entire culture or bath application of BDNF (100 ng/ml, 15 min) significantly increased the number of FM puncta that can be destained by high K^+ (Figure 5). To examine whether these increased FM puncta are juxtaposed with postsynaptic elements, we immunostained cultures with an antibody of PSD-95 (Figure 5F), a glutamatergic postsynaptic scaffolding protein. We found that 46.4% ± 23.3% (n = 58) and 34.5% ± 15.8% (n = 47) of new FM puncta induced by EFS and BDNF were colocalized with PSD-95 clusters, respectively. Similar to the TBS- or BDNF-induced conversion detected by whole-cell recording, EFS- or BDNF-induced increase in FM puncta could be prevented by pretreatment of cultures with Toxin B, K252a, or Cyt D (Figure 5G). Treatment of cultures with APV also significantly reduced EFS-induced increase in the number of FM puncta (Figure 5G). Finally, after EFS stimulation, additional perfusion with BDNF did not cause further increase in the number of FM puncta (Figure 5G), consistent with the notion that EFS and BDNF activate a common signaling pathway in the conversion process.

The EFS- or BDNF-induced increase in FM puncta may result from the mobilization of vesicles to presynaptic terminals or from the increased exocytosis of preexisting immature vesicles. To clarify these possibilities, we immunostained cultures with anti-SNP and measured the percentage of SNP-positive puncta that colocalized with FM dye puncta. As shown in Figure 6, this percentage was 91.5% ±16.7% in unstimulated old cultures and 41.3% ± 7.8% in unstimulated young cultures. EFS significantly increased the percentage to 73.5% ± 6.2% in young cultures, suggesting that enhanced exocytosis of preexisting immature synaptic vesicles is responsible, at least in part, for the EFS-induced increase in functional presynaptic terminals.

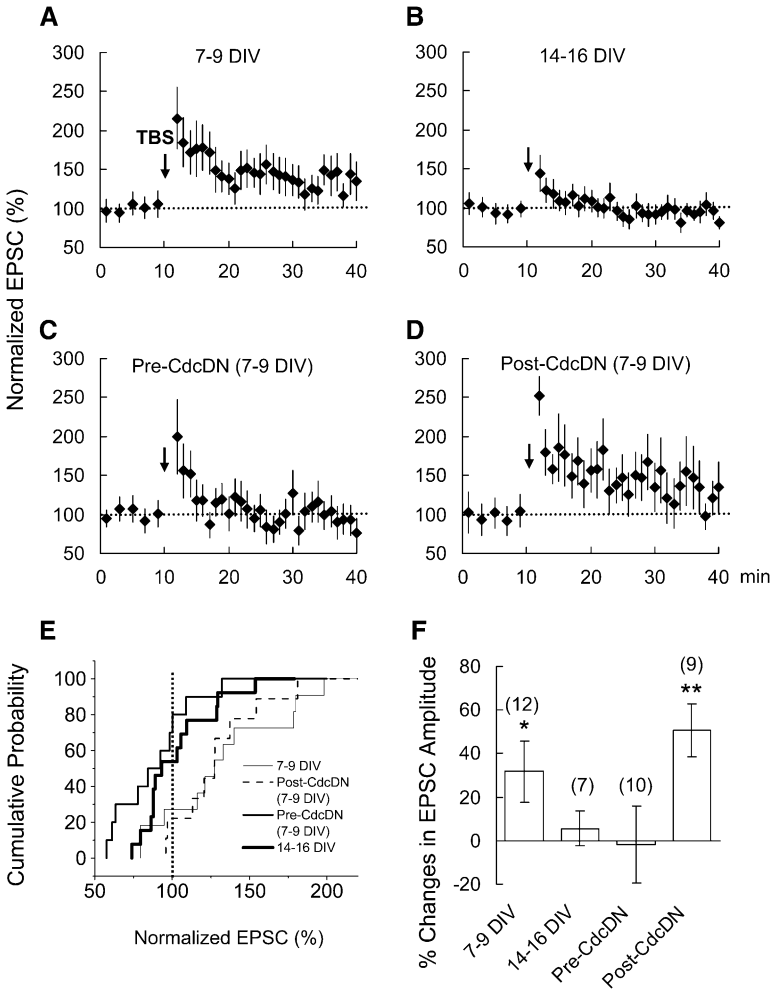

Figure 4. Effects of TBS on Efficiency of EPSCs Recorded in Young and Old Cultures

(A–D) Time course of the averaged amplitudes of EPSCs recorded before and after TBS applications (indicated by arrows) in control young (A) and old (B) cultures and in young cultures transfected with DN-Cdc42 in pre- (C) and postsynaptic (D) neurons. Data are normalized with averaged EPSC amplitude before TBS application (the first 10 min recording) for each recording.

(E) Cumulated distribution of EPSC amplitudes averaged during the period after TBS application. Data are normalized with the averaged EPSC amplitudes (dotted line) before TBS application for each recording. (F) Summary of results showing averaged percent changes in EPSC amplitudes after TBS under various conditions. The number associated with each column refers to the number of cell pairs examined in each condition. *$p < 0.05$, **$p < 0.01$, as compared with control EPSC amplitude level before TBS application.

Error bars show SEM.

Synapses at early development stages may not be functional due to the lack of readily releasable pool (RRP) of vesicles (Mozhayeva et al., 2002). To investigate whether EFS- or BDNF-induced functional presynaptic terminals involves changes in RRP, we examined the ultrastructural organization of vesicle pools under different conditions. The active zone length per terminal, the number of docked vesicles (RRP, vesicles located within 50 nm from the active zone) per active zone length (μm), and the number of vesicles in the reserve pool (RP) per terminal in the single EM sections were counted. As shown in Figure S1 in the Supplemental Data, both RRP and RP in young cultures (7 DIV) are significantly smaller than that in matured cultures (16 DIV). Treatment of young cultures with EFS or BDNF resulted in a significant increase in the RRP but not in RP (Figure S1B) and active zone length (data not shown).

Neuronal Activity Rapidly Increases Actin Polymerization at Axon Boutons

Since the actin-depolymerizing agent Cyt D abolished activity-induced functional synapses (Figures 3C and 5G), we next directly examined whether EFS can modulate actin activity. Synaptic actin localization was visualized in cultured hippocampal neurons by transfection with YFP-linked G-actin (actin-YFP). The YFP can be incorporated into the endogenous F-actin, and the fluorescent signal reflects the distribution of both F-actin and G-actin pool (Colicos et al., 2001; Dillon and Goda, 2005; Sankaranarayanan et al., 2003). Actin-YFP signal is not only concentrated in dendritic spines but also in axon boutons, where it may reflect the F-actin network that forms the scaffold for synaptic vesicle clusters (Colicos et al., 2001; Dillon and Goda, 2005; Sankaranarayanan et al., 2003). In neurons transfected with actin-YFP, fluorescent puncta can be clearly detected at axon varicosities that may potentially function as presynaptic terminals, as revealed by its colocalization with FM4-64 staining (Figure 7A) (Colicos et al., 2001; Dillon and Goda, 2005; Sankaranarayanan et al., 2003). After EFS, the YFP fluorescent intensity in axon boutons significantly increased while that in axon segments adjacent to the boutons decreased rapidly (Figures 7A and 7D), suggesting that diffusely distributed G-actin in the axon became depleted by polymerization into F-actin in the boutons. Furthermore, EFS-induced changes in the YFP fluorescence intensity in both axon boutons and axon segments were prevented by the Cyt D treatment (Figures 7E and 7G), further confirming the involvement of actin polymerization in activity-induced redistribution in YFP fluorescence.

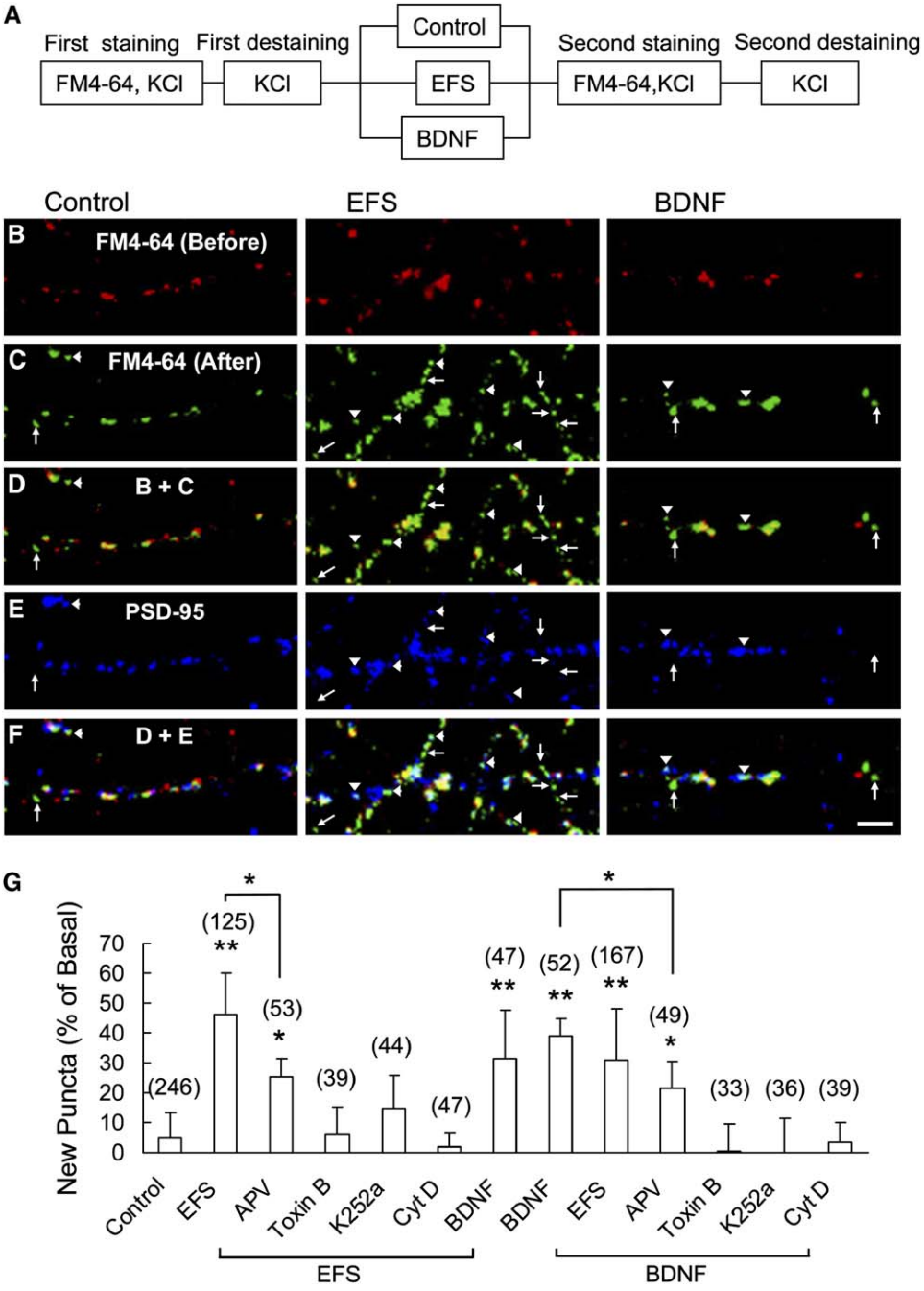

Figure 5. Rapid Increase in Functional Presynaptic Terminals Induced by EFS and BDNF

(A) Schematic illustration showing FM4-64 staining and destaining protocols to estimate functional presynaptic terminals (see Experimental Procedures for a detailed description).

(B and C) Example FM4-64 fluorescence images showing functional presynaptic terminals labeled by FM4-64 staining in 7 DIV neurons before (B) and after (C) treatment with shame (control, left column), EFS (middle column), and BDNF (100 ng/ml, 15 min, right column).

(D) Superimposed images of (B) and (C). Note the apparent increase in new puncta (pure green puncta, indicated by arrows and arrowheads) in EFS- and BDNF-treated cultures.

(E) Retrospective immunostaining of the same region as in (A) and (B) with antibody against the postsynaptic marker PSD-95.

(F) Superimposed images of (D) and (E). Note that increased new puncta with (arrowheads) or without (arrows) postsynaptic appositions (PSD-95). Images in each column from (B) to (F) are from the same microscopic field. Scale bar, 5 μm.

(G) Summary of data showing effects of various treatments on the EFS- or BDNF-induced increase in functional release sites (new FM dye puncta). Data are presented as the percent increase in FM puncta as compared to the basal level of FM puncta before induction (first staining). The number associated with each column refers to the number of image fields examined for each condition. *$p < 0.05$, **$p < 0.001$, as compared with control group or compared between two groups indicated.

Error bars show SEM.

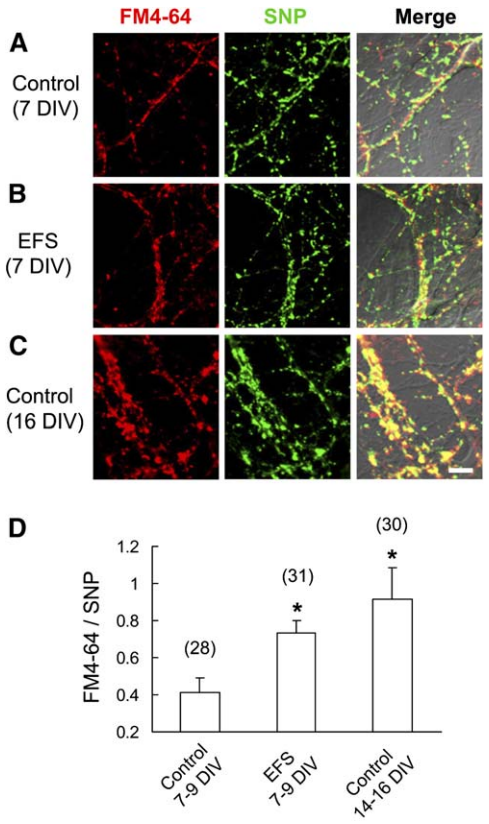

Figure 6. Comparing the Ratio of Functional (FM4-64 Puncta)/Anatomic (SNP Immunopositive Puncta) Presynaptic Terminals

(A–C) Example images showing colocalization of FM4-64 fluorescence (red) and SNP immunopositive (green) puncta obtained from 7 DIV neurons (A), 7 DIV neurons after EFS application (B), and 16 DIV neurons (C).

(D) Summarized data of the colocalization ratio of FM4-64/SNP clusters as shown in (A) to (C). The number associated with each column refers to the number of image fields examined in each condition. *$p < 0.01$ as compared with 7 DIV control group.

Error bars show SEM.

Based on FM4-64 staining, boutons were classified into three types. Type A boutons (indicated by arrowheads in Figures 7A and 7B) are stained with FM4-64 only after EFS and thus correspond to newly induced functional presynaptic terminals. Type B boutons (indicated by the red arrow and open triangle in Figures 7A and 7B) are stained with FM4-64 before as well as after EFS and may correspond to relatively matured presynaptic terminals. Type N boutons (indicated by the white arrow in Figures 7A and 7B) are not stained with FM4-64 either before or after EFS and may correspond to sites that failed to become synapses. Our analyses showed that EFS-induced increase in the YFP fluorescence intensity in type B boutons is significantly lower than that in the other two types of boutons (Figure 7D), suggesting that the actin-polymerizing activity in matured boutons (type B) is less susceptible to the regulation by neuronal activity. Immunostaining with the antibody against the presynaptic vesicle protein VAMP-2 revealed that type N boutons are deficient in the expression of the presynaptic vesicles (Figures 7A and 7B), consistent with the absence of FM4-64 staining in response to EFS.

Next we examined whether EFS-induced actin polymerization in axon boutons shares the same signaling pathway as the EFS-induced functional presynaptic terminals. We found that treatment of cultures with Toxin B or K252a prevented EFS-induced increase in the YFP fluorescence intensity in axonal boutons. Cotransfection of the cell with DN-Cdc42-myc also abolished EFS-induced changes in the YFP signal. Furthermore, perfusion with BDNF mimicked the EFS effect in inducing the increase of the YFP fluorescence intensity in these boutons (Figure 7F and 7G).

Discussion

In low-density cultures, there is a high probability of finding synaptically connected cell pairs, providing the advantage of paired whole-cell recording and selective manipulation and analysis of the properties of both pre- and postsynaptic neurons (Fitzsimonds et al., 1997; Zhang et al., 2003). Moreover, these cultures also provide an ideal system for studying functional presynaptic terminals by fluorescence imaging with FM dye. Our findings of activity-dependent conversion of nonfunctional contacts into functional synapses differ from those found for activity-induced unsilencing of "silent synapses" which exhibit NMDAR- but not AMPAR-mediated transmission. Unsilencing of synapses involves postsynaptic addition of AMPARs, whereas activity-induced conversion found in the present study depends on rapid presynaptic maturation that allows efficient glutamate release in response to electrical stimulation, a process triggered by the reorganization of actin cytoskeleton. It remains to be studied in the future whether similar mechanisms found in the present study from cultured neurons are involved in the activity-dependent synaptogenesis and synaptic maturation in intact brain tissue.

Activity-Induced Unsilencing through Rapid Presynaptic Maturation

Growth cones of many types of cultured neurons can release neurotransmitters even before contacting their targets (Young and Poo, 1983; for review see Ziv and Garner, 2004). In primary cultures of rat hippocampal neurons, functional synapses were detected several days after axodendritic contacts had been established, suggesting that presynaptic axon boutons in the vertebrate CNS undergo a slow maturation process after contacting with dendritic targets (Ziv and Garner, 2004; but see Krueger et al., 2003). The slow time course of presynaptic maturation may be attributed to the delayed expression of calcium channels, low-affinity calcium sensors, or undefined dendritic maturation factors (Ziv and Garner, 2004). Besides the well recognized morphological characteristics, e.g., clustering of vesicles and formation of active zone structure, presynaptic maturation is associated with changes in functional properties, including changes in various cytoplasmic components of presynaptic transmitter secretion machinery (Dillon and Goda, 2005; Gasparini et al., 2000; Lee and Sheng, 2000; Renger et al., 2001; Ziv and Garner, 2004), a process that may take days or even weeks to complete (Dillon and Goda, 2005; Lee and Sheng, 2000; Renger et al., 2001; Ziv and Garner, 2004).

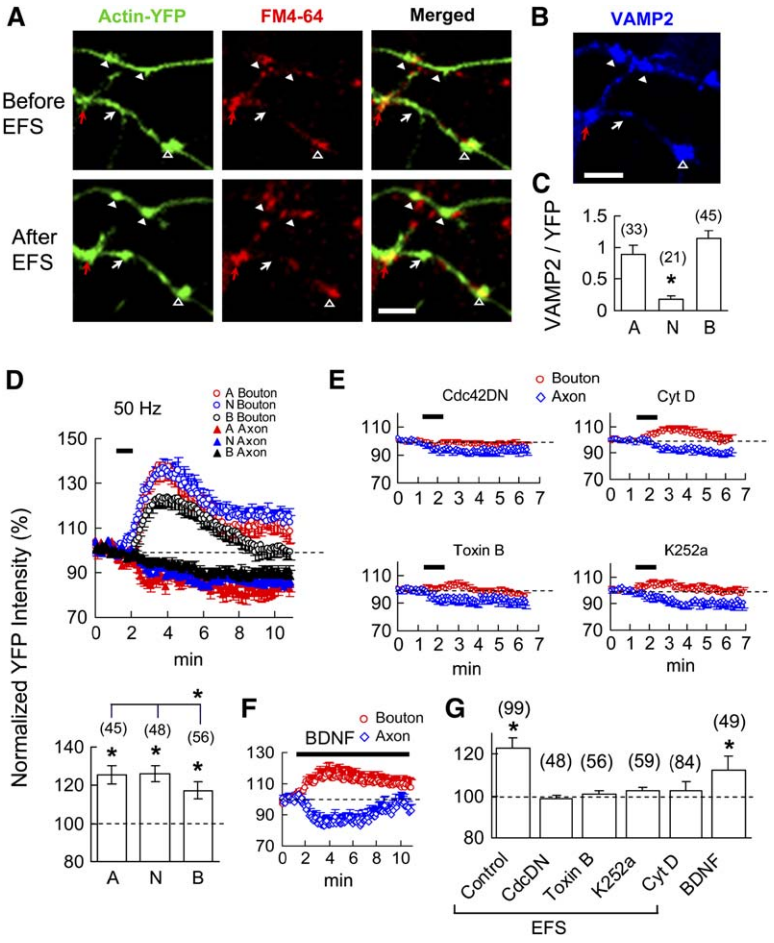

Figure 7. Activity-Induced Actin Recruitment to Axonal Boutons

(A) Example images showing axonal boutons that were transfected with actin-YFP (green, left panel) and stained with FM4-64 (red, middle panel) before (upper panels) and after (lower panels) application of EFS. The overlay (right panel) shows the colocalization of actin-YFP puncta with FM4-64 clusters. All images were from the same microscope field. Scale bar, 5 μm.

(B) The same image field as in (A) showing retrospective immunostaining with the antibody against the presynaptic vesicle protein VAMP-2. Boutons with significant increase in actin-YFP fluorescence intensity after EFS are classified into three types, each marked with different symbols (based on their labeling with FM4-64 or VAMP-2): Type "A" (arrowheads), labeled by FM4-64 after EFS. Type "B" (red arrows), labeled by FM4-64 before EFS. Type "N" (white arrows), not labeled by FM4-64 either before or after EFS. Note that N type boutons also lack apparent VAMP-2 staining, as shown in (B). Open triangles, boutons without apparent increase in fluorescence intensity of either YFP-actin or FM4-64 signal after EFS.

(C) Summarized data showing the ratio of YFP-actin/VAMP-2 signals in three types of boutons as marked in (B).

(D) Upper panel, time courses of the changes of average actin-YFP fluorescence in axonal boutons (open circles) or segments (filled triangles) in response to EFS. Bars indicate periods of EFS application. Lower panel, summary of data on EFS-induced changes in actin-YFP fluorescence of three types of boutons as shown in the upper panel. Data are averaged from the period between 2 and 4 min after the initiation of EFS. Data in both the upper and lower panels are normalized for each terminal by the average control intensity obtained during the first 70 s of imaging (dotted lines, before EFS application). "A," "B," and "N" are as defined in (B).

(E) The time courses of the changes in the average actin-YFP fluorescence in axonal boutons (red circles) or segments (blue diamonds) in response to EFS in the presence of DN-Cdc42-myc, Cyt D, Toxin B, or K252a. Data are normalized as in (D).

(F) The time course of the changes in the average actin-YFP fluorescence in axon boutons (red circles) or segments (blue triangles) in response to BDNF perfusion.

(G) Summary of data on EFS- or BDNF-induced changes in actin-YFP fluorescence in axonal boutons under different treatments as shown in (D), (E), and (F). For the DN-Cdc42 group, data are averaged for neurons cotransfected with myc-tagged DN-Cdc42 that was confirmed by immunostaining with anti-myc antibody. The number associated with each column in (C), (D), and (G) refers to the number of neurons examined in each condition. *$p < 0.05$, as compared to control (before EFS application) or between groups indicated by the line.

Error bars show SEM.

The most extensively studied silent synapses are "deaf " synapses containing only postsynaptic NMDAR but not functional AMPAR. Rapid conversion of such silent synapses through insertion of functional AMPARs at the postsynaptic membrane has been linked with the expression of LTP (Malinow and Malenka, 2002; Nicoll, 2003). Alternative hypotheses for such NMDAR-only synapses involve the glutamate spillover from neighboring active synapses to the synapses deficient in presynaptic release (Kullmann and Asztely, 1998) or a slow glutamate release through small vesicular release pores (Choi et al., 2003; Renger et al., 2001) that is selectively detected by the high-affinity NMDARs. In the present study we did not detect any NMDAR-mediated synaptic responses even in the Mg^{2+}-free extracellular solution between the cultured neurons making nonfunctional contacts. Thus, the silent synapses may arise from the deficiency in the presynaptic release mechanism or the lack of both NMDARs and AMPARs in the postsynaptic cell. Although we cannot exclude the possibility that incorporation of AMPARs to the postsynaptic membrane is involved in the TBS- or BDNF-induced functional synapses, several lines of evidence indicate that maturation in presynaptic vesicular release mechanisms was largely responsible for the activity-induced rapid conversion of silent synapses. First, the unsilencing can be prevented by treatments that selectively interfere with presynaptic functions, including loading with high concentration EGTA (Figure 1F) and transfection with TrkB·T1 (Figure 2D) or DN-Cdc42 (Figure 3C). Second, the induced functional synaptic transmission exhibited frequent failures (Figures 1B, 2B, 2C, 3A, and 3B), a phenomenon that is difficult to be explained by changes only in the postsynaptic glutamate receptors. Third, using FM labeling of functional synapses, we found that in young cultures (7 DIV) fewer SNP-positive puncta were

costained with FM dye than older cultures (Figure 6), indicating that in young cultures many presynaptic terminals are nonfunctional. Finally, application of EFS or BDNF to the young cultures rapidly induced the fraction of FM-labeled SNP puncta in young cultures to a level comparable to that in old cultures (Figure 6), further suggesting that induced functional synapses are mainly derived from conversion of previously existing silent presynaptic terminals (SNP-positive but FM-negative), rather than the formation of new terminals. Similar susceptibility to pharmacological agents for the TBS- or BDNF-induced EPSCs and FM puncta also support the notion that functional synapses detected by electrophysiological recording and by fluorescent FM imaging reflect the same cellular process. It should be noted that the fraction of TBS- or BDNF-induced functional synapses detected by patch recordings (about 15%, Figures 1F and 2D) is much lower than the induced functional presynaptic terminals revealed by FM dye imaging (about 40%, Figure 6D). It is very likely that many nonfunctional pairs recorded actually had no axon-dendritic contacts between the cells. Furthermore, functional synaptic connections detected by patch recordings require maturation of both presynaptic terminals and postsynaptic components, whereas functional presynaptic terminals detected by FM dye imaging may not be accompanied by matured postsynaptic components. This was suggested by the finding that 53.6% of EFS- and 65.5% of BDNF-induced new FM puncta have no postsynaptic apposition of PSD-95 (Figures 5F and 5G). While presynaptic maturation is clearly involved, we cannot exclude the possibility that the TBS- and BDNF-induced unsilencing also involves induction of postsynaptic maturation, e.g., increased clustering of AMPARs. Treatment of hippocampal cultures with glutamate has been reported to induce rapid increase in both presynaptic SNP clusters and postsynaptic GluR1 receptor clusters, an effect that can be also blocked by NMDAR antagonist APV or actin-depolymerizing agent Cyt D (Antonova et al., 2001), similar to our findings on the TBS-induced conversion of silent synapses (Figures 1F, 2D, 3C, and 5G). The results that NMDAR antagonist APV prevented TBS- or BDNF-induced functional synaptic transmission (Figures 1F and 2D) but only partially inhibited these stimuli-induced FM puncta (Figure 5G) further suggest that the induction of postsynaptic maturation is more strictly dependent on the activation of NMDARs.

NMDAR Activation and $[Ca^{2+}]_i$ Elevation

The NMDAR plays a key role in activity-dependent synaptic plasticity (Malinow and Malenka, 2002; Nicoll, 2003). The location of NMDARs activated by TBS is not clear, since no NMDAR-mediated synaptic responses could be detected at the converted silent synapse before TBS application. Several possibilities may exist. First, before TBS induction, the density of activated NMDARs in the postsynaptic membrane may be too low (due to low receptor density or low level of glutamate release) to be detected by the whole-cell recording method, but still high enough for inducing the conversion of the silent synapses upon TBS induction. The noise level of our recording system allowed us to detect EPSCs with amplitudes >3 pA. We could decrease the noise level to about 1 pA by averaging multiple evoked responses. Furthermore, in some experiments we optimized our recording system to achieve a noise level <2 pA. However, under all these conditions we did not detect any EPSC before the conversion by TBS (Figure S2). Second, activation of NMDARs in presynaptic terminals (Duguid and Smart, 2004), which cannot be detected by whole-cell recording at the cell body, may be responsible for the TBS-induced conversion of the silent synapses. The source of glutamate for activation of NMDARs mentioned above may come either from a low level of vesicular release or nonvesicular release, e.g., reversal of glutamate uptake (Kanai and Hediger, 2003) evoked by TBS-associated membrane depolarization. It is also possible that the release probability of the "silent" synapse is too low for the low-frequency stimulation (test pulse) to be effective in triggering synaptic transmission. Sufficient glutamate release could be triggered by the high-frequency stimulation (TBS), which in turn activates pre- or postsynaptic NMDARs and converts the stimulated synapses into functional ones. Evidence that supports this hypothesis is that EPSCs were frequently observed during TBS (Figure S3). The results that both pre- and postsynaptic Ca^{2+} elevation are critical for the TBS- and BDNF-induced conversion (Figures 1F and 2D) suggest that the retrograde signaling across the synapse (Du and Poo, 2004; Fitzsimonds et al., 1997; Micheva et al., 2003) is required for the TBS-induced presynaptic modification.

Actin Remodeling and Activity-Induced Conversion of Silent Synapses

Tetanic stimulation that induces LTP rapidly increases (within 40 s) the ratio of F-actin/G-actin in spines (Okamoto et al., 2004) and causes striking actin remodeling in the axons, including the formation of new varicosities and actin puncta as well as an increased F-actin polymerization at existing boutons (Figure 7) (Colicos et al., 2001; Dillon and Goda, 2005; Sankaranarayanan et al., 2003). The activity-dependent increase in synaptic actin puncta also depends on activation of NMDA receptors (Colicos et al., 2001), suggesting that mechanisms similar to those in LTP induction are involved. Consistent with these results, we found that stimuli (EFS, BDNF) inducing presynaptic maturation also caused actin polymerization in the axonal boutons (Figure 7). Treatments that interfered with BDNF-Cdc42 signaling prevented both the activity-induced presynaptic maturation (Figures 2, 3, and 5) and actin polymerization in these boutons (Figure 7). Furthermore, treatment with actin-depolymerizing agent Cyt D abolished activity-induced presynaptic maturation (Figures 3C and 5G). Thus, activity-induced rapid maturation of presynaptic terminals is mediated by actin polymerization in the axonal boutons.

Multiple roles have been attributed to actin filaments in synaptic transmission (Dillon and Goda, 2005; Doussau and Augustine, 2000). Dynamic RP of synaptic vesicles is anchored on actin filaments via synapsin and is recruited after rapid depletion of the RRP of synaptic vesicles (Dillon and Goda, 2005; Hilfiker et al., 1999). Actin and actin-based motor protein myosin have also been implicated in the translocation of vesicles from the RP to the RRP docked at the presynaptic plasma membrane (Dillon and Goda, 2005; Evans et al., 1998;

Prekeris and Terrian, 1997). The maturation of presynaptic boutons undergoes distinct stages (Mozhayeva et al., 2002). At the early stage, the synapses may be silent due to lack of RRP of vesicles, although they possess a recycling pool that can release neurotransmitters under strong stimulation (Mozhayeva et al., 2002). The sensitivity of activity-induced rapid conversion of silent synapses to actin-depolymerizing agent Cyt D found in the present study (Figures 3C and 5G) suggests that actin remodeling induced by TBS- or BDNF-activated Cdc42 signaling may function as an initial step in the rapid assembly of RRP at the active zone of immature synapses, enabling functional synaptic transmission following moderate physiological activity. Consistent with this notion, we found that application of EFS or BDNF significantly increased the docked synaptic vesicles (RRP) but not RP of vesicles (Figure S1). The result that EFS induced actin polymerization but failed to induce new FM puncta in boutons deficient in the expression of presynaptic vesicle protein VAMP-2 (Figures 7A to 7C) suggests that actin polymerization-mediated rapid presynaptic maturation requires the presence of RP vesicles in the presynaptic terminals.

The sensitivity of synaptic structure and function to treatment that disrupts actin polymerization depends on the extent of synapse maturation (Zhang and Benson, 2001). Actin depolymerization, while not affecting synaptic structure and function in older neurons (18 DIV), resulted in the loss of synapses in young neurons (7 DIV) and a decrease in synaptic vesicle clusters but retaining basal synaptic structure in relatively mature neurons (7–14 DIV) (Zhang and Benson, 2001). Consistent with these results, we found that treatment with Cyt D or transfection with DN-Cdc42 or TrkB·T1 in the presynaptic neurons, while not affecting basal synaptic transmission in mature synapses, abolished TBS- and BDNF-induced conversion of nonfunctional contacts into functional synapses (Figures 2D, 3C, 3D, and 3E). Thus, actin filaments play a central role in initial assembly and maintenance of synapses during early development. For matured synapse, the role of actin filaments may be replaced by the assembly of pre- and postsynaptic scaffolding proteins (Allison et al., 2000; Dillon and Goda, 2005; Ziv and Garner, 2004).

Critical Role of Cdc42 Signaling

The mechanisms underlying Cdc42-mediated rapid conversion of silent synapses remain unclear. Activation of Cdc42 signaling is responsible for 5-HT-induced long-term facilitation in *Aplysia* sensory neurons, but this induction requires several hours, suggesting involvement of different mechanisms, including substantial reorganization of the presynaptic actin network leading to the growth of new sensory neuron varicosities (Udo et al., 2005). In the present study, TBS- or BDNF-induced conversion of silent synapses occurs within minutes and is unlikely to involve protein synthesis and axon growth. Instead, Cdc42-dependent actin cytoskeleton remodeling that induces the trafficking or scaffolding of vesicles or key exocytosis molecules to the presynaptic terminal may be responsible for the activity-induced rapid conversion of silent synapses.

The Cdc42 GTPase also plays a role in regulated exocytosis (Gasman et al., 2004; Nevins and Thurmond, 2005). In particular, Cdc42 plays a key role in directing polarized secretion critical for cell polarized growth, directional migration, and selective budding (Casamayor and Snyder, 2002; Cerione, 2004; Etienne-Manneville, 2004; Wedlich-Soldner et al., 2003). The presence of the cytoskeletal matrix in the active zone is thought to facilitate the translocation of synaptic vesicles to the active zone and define the site of synaptic vesicle docking and fusion (Dillon and Goda, 2005; Ziv and Garner, 2004). It is possible that during early synaptogenesis, actin remodeling by the Cdc42 signaling cascade plays an important role for this polarized transport of synaptic vesicles to the active zone. In addition, Cdc42 signaling cascades may facilitate the transport of "piccolo/bassoon transport vesicles" or "active zone precursor vesicles" to the presynaptic site for the assembly of active zones and cytoskeletal matrix implicated in synaptic vesicle exocytosis (Li and Sheng, 2003; Shapira et al., 2003; Ziv and Garner, 2004).

Involvement of Endogenous BDNF

BDNF plays an essential role in LTP induction, probably through a presynaptic mechanism (Lu, 2003; Zakharenko et al., 2003; but see Itami et al., 2003; Kovalchuk et al., 2002). Interestingly, application of BDNF in hippocampal cultures preferentially potentiates immature synapses with a lower release probability without affecting nearby more mature synapses (Berninger et al., 1999; Lu, 2003). The most effective stimulus for inducing BDNF secretion is the LTP-inducing stimulation (Gartner and Staiger, 2002; Lu, 2003). Our results that TBS-induced unsilencing (Figure 2) and EFS-induced functional presynaptic terminals (Figure 5) can be blocked by treatments interfering with BDNF-TrkB signaling pathway suggest that activity (TBS or EFS)-induced rapid synaptic maturation is mediated by BDNF secretion. Although extensively studied, the mechanisms of BDNF effects on synaptic plasticity and synaptogenesis are still not clear (Lu, 2003). Activation of TrkB receptor is known to couple to several signaling pathways including small G proteins, MAP kinase, PI 3-kinase, and PLC-γ (Huang and Reichardt, 2003; Lu, 2003). In the present study we found that TBS- and EFS-induced conversion of silent synapses depends on activation of both BDNF and Cdc42 signaling and that BDNF-induced functional synapses can be abolished by treatments interfering with Cdc42 signaling, indicating that Cdc42 is the downstream pathway of BDNF-TrkB signaling in mediating activity-dependent presynaptic maturation and plasticity.

Experimental Procedures

Cell Culture and Transfection

Chemicals and media were from Sigma unless otherwise noted. The use and care of animals follows the guideline of the Shanghai Institutes for Biological Sciences Animal Research Advisory Committee. Hippocampal cultures were prepared as described previously (Zhang et al., 2003) with some modifications. Briefly, whole brains were isolated from embryonic day 18 SD rats, and the hippocampi were dissected out and treated with 0.25% trypsin at 37ºC for 20 min. Cells were suspended with DMEM medium (Invitrogen) containing 10% fetal bovine serum (HyClone, Logan, UT) and 10% F-12 (Invitrogen) and were plated at a density of 65,000 cells/cm^2 on poly-D-lysine-coated 35 mm dishes (Costar). Twenty-four hours after plating, half of the medium was changed to serum-free Neurobasal

(NB) medium with 2% B27 supplement (Life Technologies, Gaithersburg, MD) and 0.25% glutamine. Thereafter, half of the medium was replaced twice a week with NB medium containing 2% B27 supplement, 0.25% glutamine. After 5 days in vitro, glial cell proliferation was inhibited by exposure to 2–4 μM cytosine arabinoside.

Calcium phosphate transfection with Actin-YFP (BD Biosciences, Clontech, Palo Alto, CA), TrkB·T1-GFP (a gift from Dr. E. Castren), DN-Cdc42-GFP, or DN-Rac-GFP (gifts from Dr. G. Bokoch) was carried out on cultures between 5 and 6 DIV. DN-Cdc42-myc and Actin-YFP were cotransfected with a 1:1 ratio. Experiments were performed at 24–48 hr after transfection.

Electrophysiological Recordings

Dual patch recordings from cultured hippocampal neurons at 5–16 DIV were made at room temperature using an EPC-9 patch-clamp amplifier and corresponding Patchmaster software from Heka Electroniks (Germany) or two Axopatch-200B amplifiers (Axon Instruments) using pCLAMP acquisition software. Synaptic transmission was elicited at 0.03–0.05 Hz (+30 mV, 2 ms), and EPSCs were recorded with a patch electrode (2–7 MΩ tip resistance) in whole-cell recording mode and filtered at 2 kHz. Pipette solution contained (in mM) 136.5 K-gluconate, 0.2 EGTA, 10 HEPES, 9 NaCl, 17.5 KCl, 4 Mg-ATP, and 0.3 Na-GTP (raised to pH 7.3 with KOH). The extracellular solution (ECS) was a HEPES-buffered saline containing (in mM) 145 NaCl, 3 KCl, 10 HEPES, 3 $CaCl_2$, 8 glucose (pH 7.3). The series resistance was not compensated but was monitored continuously using a 5 mV voltage pulse. Recordings showing >20% change in series resistance were discarded. Inputs were considered to be silent after 25 to 50 successive failures of detectable EPSCs (<5 pA, peak amplitude) tested at 0.03–0.05 Hz. Conversion of silent synapses to functional synaptic transmission was then induced by presynaptic TBS stimulation (consisting of five trains of five pulses at 100 Hz separated by 200 ms, repeated five times with an interburst interval of 15 s) in current-clamp mode. The successful conversion was confirmed by continuous recording for at least 40 min, whereas the failure was judged by the lack of detectable EPSCs during at least 30 min of continuous recording after induction. The "success rate" of the induction is defined by the number of the induced functional pairs divided by the total non-functional cell pairs examined. TBS was always initiated within 10 min of attaining whole-cell mode in the presynaptic cell to prevent washout of a cytoplasmic factor (s) required for LTP induction. In some experiments, BAPTA (10 mM) or EGTA (20 mM) was added to one of the double-patched pipettes.

FM4-64 Loading and Unloading

FM4-64 (Molecular Probes) imaging was performed as described previously (Micheva et al., 2003), with some modifications. Unless otherwise noted, cells were continuously superfused in an ECS. To label active synapse, the cultured neurons were loaded with FM4-64 (10 μM) in high KCl (90 mM) solution for 30 s followed by washing in superfused ECS for 10 min (first staining). Images were taken before and after cells were destained in high KCl solution for 30 s (first destaining). Antagonists of ionotropic glutamate receptors, APV (50 μM) and DNQX (10 μM), were present during KCl exposures to block possible recurrent excitation and induction of activity-dependent synaptic plasticity. The culture was then treated with BDNF (100 ng/ml, 20 min; R&D Systems, Minneapolis, MN) or EFS followed by the second imaging procedure (second staining and second destaining). For control treatment, cultures were washed with ECS for 20 min, followed by the second imaging procedure. The image after FM dye destaining was subtracted from the initial image, and only those terminals containing activity-dependent releasable FM dye (about 90% of total staining) were analyzed. For some experiments, K252a (200 nM), Toxin B (10 μg/ml), or Cyt D (2 μg/ml) was applied to the culture for 30 min. All experiments were done at room temperature (~22ºC).

Immunocytochemistry

Following functional FM4-64 staining, neurons were fixed by 4% paraformaldehyde in PBS at 4ºC for 20 min and were permeabilized with 0.2% Triton X-100 in PBS for 10 min. Primary antibody against synaptophysin (1:1000, Chemicon), myc (Chemicon), VAMP-2 (1:800, Alomone, Israel), or PSD-95 (1:200, Affinity BioReagents, Golden, CO) was applied overnight at 4ºC, followed by rinses in PBS and staining with cy3 (1:1000) or FITC-conjugated secondary antibodies (1:400, Molecular Probes, Eugene, OR) at room temperature. Images of the fixed and immunolabeled neurons were aligned with corresponding FM images of the same region. Analysis was referred to the following methods of imaging and analysis.

Imaging and Analysis

Images were collected with the laser confocal microscope of Fluoview (Olympus, Japan) using a 40× oil objective. For experiments including immunocytochemistry, images were taken at a resolution of 516 × 516. The gain of the photomultiplier was adjusted to maximize the signal/noise ratio without causing saturation by the strongest signals. FM-positive puncta were selected for further analysis using custom scripts written in ImagePro Plus 5.1 (Media Cybernetics, Carlsbad, CA), based on the following criteria: the diameter of spots was between 0.1 and 0.6 μm and the fluorescence intensity was three standard deviations above the mean background. Under the bright-field microscope, the frames were carefully chosen to include nearly the same numbers of cell bodies. We measured the amount of more than 30 randomly collected (317 × 317 μm^2, 40× oil objective) regions in each independent experiment. Numbers of colocalization between FM-positive puncta and PSD-95 clusters were also measured by similar count methods.

Analysis of actin-YFP was performed on 7–9 DIV post-transfected hippocampal neurons. Coverslips were mounted in a perfusion chamber equipped with field stimulation electrodes on the stage of the confocal microscope. Unless otherwise noted, cells were perfused at room temperature in ECS. Quantitative measurements of fluorescence intensity at individual boutons and neighboring axonal regions were obtained by averaging a 4 × 4 area of pixel intensities. The fluorescence change of actin-YFP either at synaptic boutons or in axons were normalized to the starting fluorescence (F0) at individual selected region.

Statistical Analysis

Data are presented as mean ± SEM. Statistical comparisons were assessed with an ANOVA test or paired t test; $p < 0.05$ was taken as significant.

Supplemental Data

The Supplemental Data for this article can be found online at http://www.neuron.org/cgi/content/full/50/3/401/DC1/.

Acknowledgments

We thank Dr. M-m. Poo for critical comments on the manuscript and Ms C-H Wu for some technique assistance. This work was supported by grants from Major State Basic Research Program of China (G200077800) and the National Natural Science Foundation of China (30321002).

Received: September 19, 2005
Revised: February 14, 2006
Accepted: March 13, 2006
Published: May 3, 2006

References

Allison, D.W., Chervin, A.S., Gelfand, V.I., and Craig, A.M. (2000). Postsynaptic scaffolds of excitatory and inhibitory synapses in hippocampal neurons: maintenance of core components independent of actin filaments and microtubules. J. Neurosci. *20*, 4545–4554.

Antonova, I., Arancio, O., Trillat, A.C., Wang, H.G., Zablow, L., Udo, H., Kandel, E.R., and Hawkins, R.D. (2001). Rapid increase in clusters of presynaptic proteins at onset of long-lasting potentiation. Science *294*, 1547–1550.

Atwood, H.L., and Wojtowicz, J.M. (1999). Silent synapses in neural plasticity: current evidence. Learn. Mem. *6*, 542–571.

Berninger, B., Schinder, A.F., and Poo, M.M. (1999). Synaptic reliability correlates with reduced susceptibility to synaptic potentiation by brain-derived neurotrophic factor. Learn. Mem. *6*, 232–242.

Carlisle, H.J., and Kennedy, M.B. (2005). Spine architecture and synaptic plasticity. Trends Neurosci. *28*, 182–187.

Casamayor, A., and Snyder, M. (2002). Bud-site selection and cell polarity in budding yeast. Curr. Opin. Microbiol. *5*, 179–186.

Cerione, R.A. (2004). Cdc42: new roads to travel. Trends Cell Biol. *14*, 127–132.

Choi, S., Klingauf, J., and Tsien, R.W. (2003). Fusion pore modulation as a presynaptic mechanism contributing to expression of long-term potentiation. Philos. Trans. R. Soc. Lond. B Biol. Sci. *358*, 695–705.

Colicos, M.A., Collins, B.E., Sailor, M.J., and Goda, Y. (2001). Remodeling of synaptic actin induced by photoconductive stimulation. Cell *107*, 605–616.

Dillon, C., and Goda, Y. (2005). The actin cytoskeleton: Integrating form and function at the synapse. Annu. Rev. Neurosci. *28*, 25–55.

Doussau, F., and Augustine, G.J. (2000). The actin cytoskeleton and neurotransmitter release: an overview. Biochimie *82*, 353–363.

Doussau, F., Gasman, S., Humeau, Y., Vitiello, F., Popoff, M., Boquet, P., Bader, M.F., and Poulain, B. (2000). A Rho-related GTPase is involved in Ca(2+)-dependent neurotransmitter exocytosis. J. Biol. Chem. *275*, 7764–7770.

Du, J.L., and Poo, M.M. (2004). Rapid BDNF-induced retrograde synaptic modification in a developing retinotectal system. Nature *429*, 878–883.

Duguid, I.C., and Smart, T.G. (2004). Retrograde activation of presynaptic NMDA receptors enhances GABA release at cerebellar interneuron-Purkinje cell synapses. Nat. Neurosci. *7*, 525–533.

Etienne-Manneville, S. (2004). Cdc42—the centre of polarity. J. Cell Sci. *117*, 1291–1300.

Evans, L.L., Lee, A.J., Bridgman, P.C., and Mooseker, M.S. (1998). Vesicle-associated brain myosin-V can be activated to catalyze actin-based transport. J. Cell Sci. *111*, 2055–2066.

Fitzsimonds, R.M., Song, H.J., and Poo, M.M. (1997). Propagation of activity-dependent synaptic depression in simple neural networks. Nature *388*, 439–448.

Gartner, A., and Staiger, V. (2002). Neurotrophin secretion from hippocampal neurons evoked by long-term-potentiation-inducing electrical stimulation patterns. Proc. Natl. Acad. Sci. USA *99*, 6386–6391.

Gasman, S., Chasserot-Golaz, S., Malacombe, M., Way, M., and Bader, M.F. (2004). Regulated exocytosis in neuroendocrine cells: a role for subplasmalemmal Cdc42/N-WASP-induced actin filaments. Mol. Biol. Cell *15*, 520–531.

Gasparini, S., Saviane, C., Voronin, L.L., and Cherubini, E. (2000). Silent synapses in the developing hippocampus: lack of functional AMPA receptors or low probability of glutamate release? Proc. Natl. Acad. Sci. USA *97*, 9741–9746.

Hall, A. (1998). Rho GTPases and the actin cytoskeleton. Science *279*, 509–514.

Hilfiker, S., Pieribone, V.A., Czernik, A.J., Kao, H.T., Augustine, G.J., and Greengard, P. (1999). Synapsins as regulators of neurotransmitter release. Philos. Trans. R. Soc. Lond. B Biol. Sci. *354*, 269–279.

Huang, E.J., and Reichardt, L.F. (2003). Trk receptors: roles in neuronal signal transduction. Annu. Rev. Biochem. *72*, 609–642.

Humeau, Y., Popoff, M.R., Kojima, H., Doussau, F., and Poulain, B. (2002). Rac GTPase plays an essential role in exocytosis by controlling the fusion competence of release sites. J. Neurosci. *22*, 7968–7981.

Itami, C., Kimura, F., Kohno, T., Matsuoka, M., Ichikawa, M., Tsumoto, T., and Nakamura, S. (2003). Brain-derived neurotrophic factor-dependent unmasking of "silent" synapses in the developing mouse barrel cortex. Proc. Natl. Acad. Sci. USA *100*, 13069–13074.

Kanai, Y., and Hediger, M.A. (2003). The glutamate and neutral amino acid transporter family: physiological and pharmacological implications. Eur. J. Pharmacol. *479*, 237–247.

Korte, M., Carroll, P., Wolf, E., Brem, G., Thoenen, H., and Bonhoeffer, T. (1995). Hippocampal long-term potentiation is impaired in mice lacking brain-derived neurotrophic factor. Proc. Natl. Acad. Sci. USA *92*, 8856–8860.

Kovalchuk, Y., Hanse, E., Kafitz, K.W., and Konnerth, A. (2002). Postsynaptic induction of BDNF-mediated long-term potentiation. Science *295*, 1729–1734.

Kozma, R., Ahmed, S., Best, A., and Lim, L. (1995). The Ras-related protein Cdc42Hs and bradykinin promote formation of peripheral actin microspikes and filopodia in Swiss 3T3 fibroblasts. Mol. Cell. Biol. *15*, 1942–1952.

Krueger, S.R., Kolar, A., and Fitzsimonds, R.M. (2003). The presynaptic release apparatus is functional in the absence of dendritic contact and highly mobile within isolated axons. Neuron *40*, 945–957.

Kullmann, D.M., and Asztely, F. (1998). Extrasynaptic glutamate spillover in the hippocampus: evidence and implications. Trends Neurosci. *21*, 8–14.

Lee, S.H., and Sheng, M. (2000). Development of neuron-neuron synapses. Curr. Opin. Neurobiol. *10*, 125–131.

Li, Z., and Sheng, M. (2003). Some assembly required: the development of neuronal synapses. Nat. Rev. Mol. Cell Biol. *4*, 833–841.

Li, Y.X., Xu, Y., Ju, D., Lester, H.A., Davidson, N., and Schuman, E.M. (1998). Expression of a dominant negative TrkB receptor, T1, reveals a requirement for presynaptic signaling in BDNF-induced synaptic potentiation in cultured hippocampal neurons. Proc. Natl. Acad. Sci. USA *95*, 10884–10889.

Lu, B. (2003). BDNF and activity-dependent synaptic modulation. Learn. Mem. *10*, 86–98.

Malinow, R., and Malenka, R.C. (2002). AMPA receptor trafficking and synaptic plasticity. Annu. Rev. Neurosci. *25*, 103–126.

Matus, A. (2000). Actin-based plasticity in dendritic spines. Science *290*, 754–758.

Micheva, K.D., Buchanan, J., Holz, R.W., and Smith, S.J. (2003). Retrograde regulation of synaptic vesicle endocytosis and recycling. Nat. Neurosci. *6*, 925–932.

Mozhayeva, M.G., Sara, Y., Liu, X., and Kavalali, E.T. (2002). Development of vesicle pools during maturation of hippocampal synapses. J. Neurosci. *22*, 654–665.

Nevins, A.K., and Thurmond, D.C. (2005). A direct interaction between Cdc42 and vesicle-associated membrane protein 2 regulates SNARE-dependent insulin exocytosis. J. Biol. Chem. *280*, 1944–1952.

Nicoll, R.A. (2003). Expression mechanisms underlying long-term potentiation: a postsynaptic view. Philos. Trans. R. Soc. Lond. B Biol. Sci. *358*, 721–726.

Okamoto, K., Nagai, T., Miyawaki, A., and Hayashi, Y. (2004). Rapid and persistent modulation of actin dynamics regulates postsynaptic reorganization underlying bidirectional plasticity. Nat. Neurosci. *7*, 1104–1112.

Prekeris, R., and Terrian, D.M. (1997). Brain myosin V is a synaptic vesicle-associated motor protein: evidence for a Ca2+-dependent interaction with the synaptobrevin-synaptophysin complex. J. Cell Biol. *137*, 1589–1601.

Renger, J.J., Egles, C., and Liu, G. (2001). A developmental switch in neurotransmitter flux enhances synaptic efficacy by affecting AMPA receptor activation. Neuron *29*, 469–484.

Sankaranarayanan, S., Atluri, P.P., and Ryan, T.A. (2003). Actin has a molecular scaffolding, not propulsive, role in presynaptic function. Nat. Neurosci. *6*, 127–135.

Shapira, M., Zhai, R.G., Dresbach, T., Bresler, T., Torres, V.I., Gundelfinger, E.D., Ziv, N.E., and Garner, C.C. (2003). Unitary assembly of presynaptic active zones from Piccolo-Bassoon transport vesicles. Neuron *38*, 237–252.

Slutsky, I., Sadeghpour, S., Li, B., and Liu, G. (2004). Enhancement of synaptic plasticity through chronically reduced Ca2+ flux during uncorrelated activity. Neuron *44*, 835–849.

Udo, H., Jin, I., Kim, J.H., Li, H.L., Youn, T., Hawkins, R.D., Kandel, E.R., and Bailey, C.H. (2005). Serotonin-induced regulation of the actin network for learning-related synaptic growth requires Cdc42, N-WASP, and PAK in Aplysia sensory neurons. Neuron *45*, 887–901.

Vicario-Abejon, C., Collin, C., McKay, R.D., and Segal, M. (1998). Neurotrophins induce formation of functional excitatory and inhibitory synapses between cultured hippocampal neurons. J. Neurosci. *18*, 7256–7271.

Wedlich-Soldner, R., Altschuler, S., Wu, L., and Li, R. (2003). Spontaneous cell polarization through actomyosin-based delivery of the Cdc42 GTPase. Science *299*, 1231–1235.

Young, S.H., and Poo, M.M. (1983). Spontaneous release of transmitter from growth cones of embryonic neurones. Nature *305*, 634–637.

Yuan, X.B., Jin, M., Xu, X., Song, Y.Q., Wu, C.P., Poo, M.M., and Duan, S. (2003). Signalling and crosstalk of Rho GTPases in mediating axon guidance. Nat. Cell Biol. *5*, 38–45.

Zakharenko, S.S., Patterson, S.L., Dragatsis, I., Zeitlin, S.O., Siegelbaum, S.A., Kandel, E.R., and Morozov, A. (2003). Presynaptic BDNF required for a presynaptic but not postsynaptic component of LTP at hippocampal CA1-CA3 synapses. Neuron *39*, 975–990.

Zhang, W., and Benson, D.L. (2001). Stages of synapse development defined by dependence on F-actin. J. Neurosci. *21*, 5169–5181.

Zhang, J.M., Wang, H.K., Ye, C.Q., Ge, W., Chen, Y., Jiang, Z.L., Wu, C.P., Poo, M.M., and Duan, S. (2003). ATP released by astrocytes mediates glutamatergic activity-dependent heterosynaptic suppression. Neuron *40*, 971–982.

Zhang, H., Webb, D.J., Asmussen, H., Niu, S., and Horwitz, A.F. (2005). A GIT1/PIX/Rac/PAK signaling module regulates spine morphogenesis and synapse formation through MLC. J. Neurosci. *25*, 3379–3388.

Ziv, N.E., and Garner, C.C. (2004). Cellular and molecular mechanisms of presynaptic assembly. Nat. Rev. Neurosci. *5*, 385–399.